Vaccination against nonmutated neoantigens induced in recurrent and future tumors

Garrido, G.; Schrand, B.; Levay, A.; Rabasa, A.; Ferrantella, A.; Silva, D.M. da; ... ; Gilboa, E.

Vaccination against Nonmutated Neoantigens Induced in Recurrent and Future Tumors

Greta Garrido[1], Brett Schrand[1], Agata Levay[1], Ailem Rabasa[1], Anthony Ferrantella[2], Diane M. Da Silva[3], Francesca D'Eramo[1], Koen A. Marijt[4], Zhuoran Zhang[5], Deukwoo Kwon[6], Marcin Kortylewski[5], W. Martin Kast[3], Vikas Dudeja[2,7], Thorbald van Hall[4], and Eli Gilboa[1,7]

ABSTRACT

Vaccination of patients against neoantigens expressed in concurrent tumors, recurrent tumors, or tumors developing in individuals at risk of cancer is posing major challenges in terms of which antigens to target and is limited to patients expressing neoantigens in their tumors. Here, we describe a vaccination strategy against antigens that were induced in tumor cells by downregulation of the peptide transporter associated with antigen processing (TAP). Vaccination against TAP downregulation–induced antigens was more effective than vaccination against mutation-derived neoantigens, was devoid of measurable toxicity, and inhibited the growth of concurrent and future tumors in models of recurrence and premalignant disease. Human $CD8^+$ T cells stimulated with TAP^{low} dendritic cells elicited a polyclonal T-cell response that recognized tumor cells with experimentally reduced TAP expression. Vaccination against TAP downregulation–induced antigens overcomes the main limitations of vaccinating against mostly unique tumor-resident neoantigens and could represent a simpler vaccination strategy that will be applicable to most patients with cancer.

Introduction

Neoantigen burden, mostly corresponding to randomly arising nonsynonymous mutations in tumor cells, is a major determinant of tumor immunogenicity, underscored by clinical studies showing that responsiveness to checkpoint blockade therapy correlates with the number of neoantigens expressed in the patients' tumor. Yet, most patients do not express, or express too few, tumor-resident mutation-derived neoantigens (1–3). Neoantigens expressed in a recurring tumor, a main challenge in clinical oncology (4–6), may differ from the neoantigens isolated from a tumor biopsy month or years earlier (7–11), and the question of which neoantigens will be expressed in tumors that will emerge in individuals at risk of developing cancer cannot be predicted (12).

Here, we describe a vaccination approach against antigens induced in concurrent, recurring, or future tumors by transient downregulation of the transporter-associated with antigen processing (TAP), which overcomes the aforementioned limitations of targeting tumor-resident mutation-generated neoantigens. Downregulation of TAP in tumor cells induces the presentation of class I–restricted epitopes, termed T-cell epitopes associated with impaired peptide processing (TEIPP; ref. 13), that can elicit T-cell responses and inhibit the growth of TAP-deficient tumors (13–16, reviewed in ref. 17). Importantly, every tumor cell in which TAP is downregulated will present a common set of new antigens (13, 14, 17, 18) corresponding to the rare but clinically relevant mutation-derived clonal neoantigens expressed in tumors (19–22).

We previously showed that tumor-targeted transient downregulation of TAP, using a corresponding siRNA targeted to tumor cells *in vivo* by conjugation to a broad-range nucleolin binding aptamer (Nucl), induces the presentation of TEIPP in the tumor cells and inhibits tumor growth in multiple murine tumor models of distinct origin in the absence of measurable toxicity (23). In this study, we tested the hypothesis that vaccination against TEIPP induced by TAP downregulation could enhance the antitumor response elicited against the TEIPP-presenting tumor cells, and describe a simple and broadly applicable vaccination strategy whereby a TAP-specific siRNA was targeted to dendritic cells (DC) *in vivo* by conjugation to a CpG oligonucleotide (ODN; ref. 24). Vaccination against induced antigens resulting from TAP downregulation is also suitable for recurrent and future tumors because it eliminates the uncertainties associated with vaccination against tumor-resident neoantigens (7–11).

Materials and Methods

Cells

A20 and 4T1 cell lines were purchased from ATCC in 2002–2004, and Ramos, MRC-5, SW620, and SW480 cells were purchased from ATCC in 2016–2017. MC38 cells were purchased from Kerafast in 2002–2004. The DC2.4 mouse DC line was purchased from Millipore Sigma in 2014. 67NR, RMA, RMA-S (TAP2-deficient), and RMA-S expressing B7-1 molecules (RMA-S-B7) described before (13, 18) were obtained from T. van Hall (Leiden University Medical Center, Leiden, the Netherlands) in 2015. HLA-$A^*02:01^+$ 518A2 melanoma and its TAP1 knock-out variant generated by CRISPR/CAS9 technology has

[1]Department of Microbiology and Immunology, University of Miami, Miller School of Medicine, Miami, Florida. [2]Department of Surgery, University of Miami, Miller School of Medicine, Miami, Florida. [3]Norris Comprehensive Cancer Center, University of Southern California, Los Angeles, California. [4]Department of Medical Oncology, Oncode Institute, Leiden University Medical Center, Leiden, the Netherlands. [5]Department of Immuno-Oncology, Beckman Research Institute, City of Hope Medical Center, Duarte, California. [6]Department of Public Health Sciences, University of Miami, Miller School of Medicine, Miami, Florida. [7]Sylvester Comprehensive Cancer Center, University of Miami, Miller School of Medicine, Miami, Florida.

Note: Supplementary data for this article are available at Cancer Immunology Research Online (http://cancerimmunolres.aacrjournals.org/).

G. Garrido and B. Schrand contributed equally to this article.

Corresponding Author: Eli Gilboa, University of Miami Miller School of Medicine, 1550 NW 10th Avenue, Miami, FL 33136. Phone: 305-243-1767; Fax: 305-243-4409; E-mail: egilboa@med.miami.edu

Cancer Immunol Res 2020;8:856–68

doi: 10.1158/2326-6066.CIR-20-0020

been previously described (25) and was obtained from T. van Hall (Leiden University Medical Center, Leiden, the Netherlands) in 2017. The human B-cell lymphoma cell line TMD8 was kindly provided by Dr. Marcin Kortylewsky in 2018. HPV16-transformed mouse and human TC-1, B6 HLF CASKI, and C33a cells were kindly provided by W. Martin Kast (University of Southern California, Los Angeles, CA) in 2018. The isolation and culture of cells derived from primary KPC tumors and pancreatic stellate was described before (26). The generation and culture of mouse $CD8^+$ T-cell clone LnB5, with specificity for the TRH4-derived peptide in the context of H-2Db, and the generation and expansion of human $CD8^+$ T-cell clone 1A8, specific for the LRPAP1-derived peptide in the context of HLA-A2, have been previously described (13, 14, 18, 25) and were obtained from T. van Hall (Leiden University Medical Center, Leiden, the Netherlands) in 2015.

De-identified peripheral blood mononuclear cells (PBMC) from $HLA\text{-}A2^+$ healthy donors were obtained from Precision for Medicine. Monocytes were isolated using human CD14 microbeads following manufacture's protocol (negative selection; Miltenyi Biotec). From the isolated fraction the 90%–98% of cells were $CD14^+$ by flow cytometry. Isolated monocytes were cultured (1×10^6 cells/mL) in 6-well plates for 6 days in the presence of GM-CSF (100 ng/mL) and IL4 (50 ng/mL; R&D Systems), yielding immature monocytes-derived DCs, which were subsequently matured as described below. Autologous $CD8^+$ T cells were also isolated from same donors using human $CD8^+$ T-cell isolation kit following manufacturer's instructions (Miltenyi Biotec), and the purity of $CD8^+$ T-cell population was 75%–85%, as determined by flow cytometry. $CD8^+$ T cells were used in coculture experiments as described below.

Cell line culture conditions

Cell lines were cultured in RPMI1640 medium (A20, 4T1, 67NR, Caski, C33A, Ramos, TMD8, TC-1, B6 HLF, and DC2.4 cells), DMEM (MC38, MRC-5, SW480, and SW620), or Iscove modified Dulbecco's medium (RMA, RMA-S, RMA-S-B7, 518A2, and the mouse T-cell activation assays described below), all from Gibco, supplemented with 8%–10% heat-inactivated FCS, penicillin (100 U/mL), and streptomycin (100 μg/mL; Gibco Life Technologies). Mouse T cells were additionally supplemented with 1 mmol/L sodium pyruvate, 0.05 mmol/L β-mercaptoethanol, and 2 mmol/L minimal essential medium (MEM) nonessential amino acids (Gibco Life Technologies). TC-1 and B6 HLF cells were additionally supplemented with 1 mmol/L sodium pyruvate, 2 mmol/L (MEM) nonessential amino acids, and gentamicin (50 μg/mL; Thermo Fisher Scientific). For TC-1 cells, G418 geneticin (0.4 mg/mL) and Hygromycin b (0.2 mg/mL) were also added (Thermo Fisher Scientific). DC and T-cell culture media, from StemCell Technologies, were used for human DC differentiation and T-cell cultures, respectively. All cell lines and assay cultures were maintained at 37°C and 5 % CO_2. All cells were tested regularly for *Mycoplasma* contamination. Cell lines were authenticated by the vendor. Cells were passaged for a limited number of cycles and discarded. Briefly, cells obtained from the vendor were passaged 4–5 times and frozen in 10–20 aliquots (F1). A frozen vial of F1 cells was thawed, passaged 4–5 times, monitored for *Mycoplasma*, and frozen in 10–20 aliquots (F2). For each experiment, F2 cells were thawed and passaged 4–7 cycles depending on the experiment.

Design of CpG–siRNA conjugates

Sequences of CpG ODNs used in the study were as follows: CpG 1668 (5′-tccatgacgttcctgatgct-3′), CpG 2006 (5′-tcgtcgttttgtcgttttgtcgtt-3′), and CpG D19 (5′-ggTGCATCGATGCAGggggg-3′). Bases in capital letters are phosphodiester; bases in lower case are phosphorothioate (nuclease resistant). These sequences were extended at the 3′ end with the following sequence (termed linker): 5′ CGAGGCUAUCUAGAAUGUAC, and were purchased from Trilink Biotechnologies. The Nucleolin aptamer (23), extended at the 3′ end with the following sequence (termed linker): 5′ GUACAUUCUAGAUAGCC, was purchased from Trilink Biotechnologies. Complementary linker sequences extending from the sense strand of murine TAP2 (5′GCUGCACACGGUUCAGAAT), murine ERAAP (5′GCUAUUACAUUGUGCAUTA), human TAP1 (5′ CAGGAUGAGUUACUUGAAA), or control (Ctrl) (5′ UAAAGAACCAUGGCUAACC) siRNAs were ordered from IDT and contained 2′ O-methyl-modified pyrimidines with the last two bases being deoxynucleotides. Antisense siRNA sequences, ordered from IDT, were as follows: murine TAP2 (5′ AUUCUGAACCGUGUGCAGCmUmU), murine ERAAP (5′ UAAUGCACAAUGUAAUAGCmUmU), human TAP1 (5′ UUUCAAGUAACUCAUCCUGmUmU), and Ctrl (5′ GGUUAGCCAUGGUUCUUUAmUmU), whereby 'm' indicated the presence of a 2′ O'-methyl–modified ribonucleotide. CpGs or the Nucleolin aptamer were annealed to duplex siRNAs in PBS at 82°C for 4 minutes or 37°C for 10 minutes, respectively, in a block heater and allowed to cool to room temperature. Bioconjugates were stored at −80°C until use.

CpG–STAT3 conjugates

The CpG type B oligonucleotide (CpG7909) was cosynthesized with a STAT3 DNA-binding site by the City of Hope Medical Center DNA/RNA core as described previously (27, 28): 5′-T*C*G*T*C*G*T*T*T*T*G*T*C*G*T*T*T*T*G*T*C*G*T*Txxxx-x-C*A*T*TTCCCGTAAATC-xxxx-GATTTACGGGAA*A*T*G-xxxxx-3′. Asterisks indicate phosphorotiate-modified nucleotides. X – $(CH2)_3$ methylene spacers.

Study approval

All animal work was conducted under the approval of the University of Miami Institutional Animal Care and Use Committee (IACUC) in accordance with federal, state, and local guidelines.

Mouse strains

All mice indicated below were purchased from The Jackson Laboratories.

Transplantable tumor models and therapy

Therapeutic regimen

C57BL/6J mice were used for RMA, MC-38, and TC-1 models. BALB/c mice were used for 4T1, 67NR, and A20 models. Seven 9-week-old female mice were injected subcutaneously (s.c.) in the right flank with RMA (5×10^4), 4T1 (2×10^4), 67NR (1×10^5), MC38 (1×10^5), A20 (7.5×10^5), or TC-1 (1×10^5) tumor cells. Two days following tumor inoculation, a single dose of CpG–siRNA conjugate at of 0.75 nmol (1.3 mg/kg) was administered s.c. close to inguinal lymph node in the right flank. When tumors became palpable (volume: 25–75 mm^3), Nucl-siRNAs were administered intraperitoneally (i.p.) at 1 nmol (1.75 mg/kg). This was repeated two additional times 3 days apart. In experiments with MC38-bearing mice, a peptide vaccination protocol was used as described previously (29). The treatment schedule for the peptide vaccine was a single dose on the same day as the first Nucl-TAP siRNA dose. For TC-1 studies, 7- to 9-week-old female mice received two injections with CpG–siRNA conjugates 1 and 7 days following tumor inoculation.

For adoptive transfer experiments, C57BL/6J mice were injected s.c. with RMA-S (1×10^6) cells. Two days after tumor implantation, mice received one infusion of $CD8^+$ T cells (0.25×10^6) from naïve mice vaccinated with CpG-siRNAs. For the generation of TAP-deficient specific $CD8^+$ T cells, C57BL/6J-naïve mice (tumor-free) that received three doses of CpG–siRNA conjugates every 10 days were euthanized 5 days after the third dose. Cells from the inguinal lymph nodes were isolated and restimulated *in vitro* for 48 hours with IL2 (20 IU/mL) in the presence of irradiated RMA-S-B7 (1:3, APC:target ratio) and autologous splenocytes (2.5:1, splenocytes:T-cell ratio). $CD8^+$ T cells were purified using a mouse $CD8a^+$ T cells isolation kit following the manufacturer's protocol (negative selection; Miltenyi Biotec). Purity of $CD8^+$ T-cell population was 85%–95% as determined by flow cytometry.

Prophylactic regimen

Seven 9-week-old female mice were injected s.c. as described before with CpG–siRNA conjugates at 0.75 nmol on days −20 and −10. At day zero, tumor cells were inoculated subcutaneously followed by a third dose of CpG-siRNAs 3 days later. For RMA and 4T1 tumor models, once tumors became palpable (volume: 25–75 mm^3), Nucl-siRNAs were administered i.p. at 1 nmol and repeated two additional times 3 days apart. For the analysis of immune cell infiltrates in 4T1-bearing mice, tumors were resected 2 days after the second dose of Nucl-siRNAs conjugates and processed as described below. Cellular subsets were depleted by administering depleting antibody i.p. once weekly beginning 3 days before first CpG-TAP siRNA administration dose: $CD8^+$ T cells with anti-CD8α (200 μg, clone 2.43, BioXCell), $CD4^+$ T cells with anti-CD4 (200 μg, clone GK1.5, BioXCell), natural killer (NK) cells with anti-asialo GM1 (20 μL, clone Poly21460, BioLegend). Depletion of $CD8^+$ T cells, $CD4^+$ T cells, and NK cells (>95%) were confirmed by flow cytometry. For the analysis of long lasting protective immunity by CpG-TAP treatment, mice were vaccinated with CpG-siRNAs at days −20 and −10, and implanted subcutaneously with RMA-S tumor cells 10 or 90 days after second treatment dose. A third dose of CpG-siRNAs was injected three days after tumor implantation. For the identification of TRH4-specific $CD8^+$ T cells in the memory population, C57BL/6J-naïve mice (tumor free) that have received three doses of CpG-siRNA conjugates subcutaneously or intraperitoneally every 10 days were euthanized 30 days after the third dose. Cells from inguinal lymph nodes or spleens were isolated and processed as described below.

For *in vivo* cytotoxicity assays, 10 days after last dose of CpG-siRNAs, syngeneic naive splenocytes were isolated and labeled with either 5 μmol/L CFSE ($CFSE^{hi}$ cells) or 0.5 μmol/L CFSE ($CFSE^{lo}$ cells; Thermo Fisher Scientific). $CFSE^{hi}$ cells were pulsed with TRH4 peptide (MCLRMTAVM), and $CFSE^{lo}$ cells were pulsed with an irrelevant peptide for $H\text{-}2D^b$ (Ad10, SGPSNTPPEI; ref. 13). Peptides were synthetized by GenScript. RMA tumor–bearing mice treated with Nucl-siRNAs as described before, or left untreated, were injected intravenously (i.v.) with 5×10^6 CFSE-labeled cells mixed at 1:1 ratio. Forty-eight hours later, spleens were harvested and CFSE-labeled cells enumerated by flow cytometry. The percentage of specific killing was calculated as follows: 1 - [(% $CFSE^{lo}$ control/% $CFSE^{hi}$ control)/(% $CFSE^{lo}$ treated/% $CFSE^{hi}$ treated)] × 100. Caliper measurements on tumors were done three times weekly, and mice were euthanized when the tumor volume exceeded 1,000 mm^3, mice exhibited signs of morbidity, or ulcerated tumors. Tumor volume was measured using the formula $W(2) \times L)/2$, where W is tumor width and L is tumor length. Experiments were terminated when two or more mice were sacrificed in the "untreated" group.

Autochthonous tumor models and therapy

Recurrence model for pancreatic cancer

Seven 9-week-old female C57BL/6J mice were anesthetized, a laparotomy was performed, and short-term cultured KPC-derived cells (2×10^3) mixed with pancreatic stellate cells (1.8×10^4) were injected into the tail of the pancreas. The pancreas was then carefully returned to the peritoneal cavity, the abdomen was closed with a 4–0 vicryl suture, and the skin was stapled. Twenty-one days later, tumors in pancreas were removed. CpG-siRNAs were administered i.p. at 0.75 nmol per dose 2 days before resection surgery and continued two times every 10 days. Nine days following tumor resection, Nucl-siRNAs were administered i.p. at 0.5 nmol per dose twice per week for three weeks. Mice were euthanized when they exhibited signs of morbidity.

Methylcholanthrene-induced sarcoma model

BALB/c 6-week-old female mice received a single intramuscular (i.m.) injection of 400 μg of the chemical carcinogen 3-methylcholanthrene (MCA, Sigma-Aldrich) dissolved in 100 μL of sterile corn oil using an insulin syringe. Development of fibrosarcomas was monitored periodically over the course of 40–201 days. Tumors >20 mm in diameter, using calipers, and demonstrating progressive growth were recorded as positive. Thirty-five days following tumor induction, CpG-siRNAs were administered i.p. at 0.75 nmol per dose and repeated two additional times 10 days apart. Once tumors became palpable, Nucl-siRNAs were administered i.p. at 0.5 nmol per dose twice per week for three weeks. Mice were euthanized when they exhibited signs of morbidity.

MMTV-PyMT model

Starting at 5 weeks old (before first spontaneous tumors developed), age-matched hemizygous MMTV-PyMT females (provided by Dr. Marc Lippman, Department of Medicine, University of Miami Miller School of Medicine, Miami, FL) received i.p. injections of 0.75 nmol CpG-siRNAs every 10 days for total of 6 doses. Once tumors started developing, Nucl–siRNA conjugates were administered i.p. at 0.5 nmol per dose twice per week for 4 weeks. Tumors in mammary glands were monitored three times weekly. Mice were euthanized when they exhibited signs of morbidity.

siRNA knockdown and qPCR analysis

For *in vitro* siRNA knockdown, DC2.4, Ramos, TMD8 cell lines, and immature human monocytes-derived DC cells were plated in triplicate onto 24-well plates ($2.5–5 \times 10^4$ cells) for 18 hours. After complete adhesion, cells were incubated with 0.5 μmol/L Nucl-siRNA or 0.3 μmol/L CpG–siRNA conjugates two times every 8 hours. Cells were harvested 24, 48, 72, or 96 hours after the last treatment. For *in vivo* siRNA knockdown, BALB/c mice were injected once s.c. with CpG-siRNAs (0.75 nmol) close to inguinal lymph nodes in the right flank. Lymph nodes were excised 24 hours later and DCs were isolated using CD11c MicroBeads (Miltenyi Biotec).

Murine *Tap2* or human *TAP1* mRNA was quantified by qPCR. RNA was isolated using an RNeasy kit (QIAGEN). RNA was quantified using an Agilent 2100 Bioanalyzer (Agilent Technologies). cDNA synthesis was performed using the High Capacity cDNA Reverse Transcription kit (Applied Biosystems). cDNA equivalents

of 25–50 ng of mRNA were used per reaction in a TaqMan qPCR assay using the Step One qPCR machine (Applied Biosystems). TaqMan probes corresponding to gene of interest or housekeeping products, ordered from Thermo Fisher Scientific, were as follows: Tap2 (Mm01277033_m1), ACTB (Mm02619580_g1), Tap1 (Hs00184465_m1), HPRT1 (Hs02800695_m1).

Generation of human CD8$^+$ T cells enriched for TAP downregulation–induced epitopes

Human DCs differentiated from monocytes, as described above, were incubated with 0.3 μmol/L CpG–siRNA conjugates two times every 24 hours. Twenty-four hours after second pulse, DCs were cocultured with homologous CD8$^+$ T cells using T-cell culture medium in presence of IL2 (20 ng/mL, R&D Systems) and IL15 (50 ng/mL, R&D Systems) for 6 days. A third pulse with CpG-siRNAs was done on the day of coculture. Culture medium was replenished every 2–3 days with fresh complete T-cell medium with cytokines. After two rounds of specific stimulation, the CD8$^+$ T cells were isolated using a positive-selection CD8$^+$ T-cell isolation kit (Miltenyi Biotec).

Recognition of targets by human TAP downregulation–induced epitope-specific CD8$^+$ T cells

CpG-siRNA– or TAP-siRNA–treated, peptide-pulsed, virus-infected, or untreated cells were cocultured with activated Lnb5 T cells, 1A8 T cells, or TAP deficiency epitope enriched CD8$^+$ T cells (E:T ratio, 1:10). Peptides (1 μg/mL) were added (purchased from Anaspec), and sequences were as follows: P14-FLGPWPAAS; P29-LLALAAGLAV; P44-FLYPFLSHL; P49-ILEYLTAEV; P9-VLAVFIKAV; P67-LSEKLERI; P32-LLLSAEPVPA; control MAGE-ALSRKVAEL. Murine or human IFNγ production in supernatant after 20 hours stimulation was measured by ELISA from R&D systems following manufacturer's instructions. Cytotoxic activity was determined in a 4-hour *in vitro* lactate dehydrogenase assay (Thermo Fisher Scientific) using E:T ratio of 10:1 in T-cell media following the manufacturer's protocol. Percentage of specific lysis was calculated as: ([experimental release − effector cell release − spontaneous release]/[maximum release − spontaneous release]) × 100.

Flow cytometry analysis

Multicolor flow cytometry staining was performed using the following antibodies and reagents: CD45-FITC (30-F11), CD3-BV785 (17A2), CD19-APC/Cy7 (6D5), CD8a-BV510 (53–6.7), CD4-AF700 (RM4-5), CD335-BV605 (29A1.4), F4/80-APC (BM8), CD11c-PE/Cy7 (N418), I-A/I-E-BV785 (M5/114.15.2), Ly-6C-PerCP/Cy5.5 (HK1.4), H-2-PE (M1/42), Ly-6G-BV605 (1A8), CD11b-PerCP/Cy5.5 (M1/70), KLRG1-APC (2F1/KLRG1), CD62L-BV711 (MEL-14), and Ly-6G-APC/Cy7 (1A8) from BioLegend. CD3-APC/Cy7 (17A2) and CD11b-redFluor710 (M1/70) were obtained from Tonbo Biosciences. CD19-PF-594 (1D3) and CD103-BV421 (M290) were obtained from BD Biosciences. CD25-PE/Cy7 (PC61.5) and Foxp3-PE (FJK-16s) were obtained from eBiosciences. The TRH4 tetramer (TRH4 Tetramer/PE H-2Db) was produced by the central protein facility of the Leiden University Medical Center (Leiden, the Netherlands). Tumor-infiltrating lymphocytes (TIL) were analyzed as described previously (30). Briefly, TILs were isolated by dissecting tumor tissue into small pieces followed by incubation in collagenase (1 mg/mL, Worthington) and DNase (100 μg/mL, Sigma-Aldrich) in complete RPMI1640 medium prior to dissociation using the gentleMACS Dissociator following manufacturer's instructions for tough tumors like those induced with the 4T1 cell line (Miltenyi Biotec). Cell suspensions were passed through a 70-μm nylon strainer to obtain a single-cell population. Cells were washed twice with FACS buffer (PBS pH 7.2, supplemented with 0.5% BSA, 2 mmol/L EDTA, and 0.09% azide) and stained as described below. Cells were incubated with Fc-blocking antibodies (purified anti-mouse CD16/32, clone 93, BioLegend) for 10 minutes at 4°C, then incubated with antibodies for 30 minutes at 4°C. CD11c$^+$ cells for DC maturation analysis or 4T1/67NR cells for MHC-I expression were processed using the same protocol. For tetramer experiments, cells were stained with the tetramer for 10 minutes at 22°C, followed by staining with antibodies. Cell suspensions were incubated with fixable viability dye eFluor780 (eBioscience) for 15 minutes at 4°C. After a washing step, cells were either analyzed directly or fixed with 4% paraformaldehyde (PFA, BD Biosciences) solution for 30 minutes and stored in a 1% PFA solution until analysis. For intracellular staining of Foxp3, cells were fixed and permeabilized with Foxp3 Staining Buffer Kit (eBioscience) according to manufacturer's instructions. Cells were analyzed using LSR II cytometer (Becton Dickinson), and data were analyzed using FlowJo 10 software (TreeStar). Cytokine concentration in serum was analyzed using a CytoFLEX flow cytometer and LEGENDplex software (BioLegend).

Toxicology

Naïve BALB/c mice were administered CpG–siRNA and Nucl–siRNA conjugates as described in the vaccination regimen in transplantable tumor models. Blood was collected from mice 2 days after last Nucl-siRNAs administration dose. Complete blood count (CBC) analysis was performed using HemaVet analyzer (Drew Scientific). Liver enzymes AST and ALT were quantified in serum by using a colorimetric Aspartate Aminotransferase Activity Assay Kit (Sigma) or Alanine Aminotransferase Activity Assay Kit (Cayman Chemical), respectively, according to the manufacturer's protocol. Cytokines were quantified in serum by LEGENDplex Mouse Inflammation panel (13-plex; BioLegend) according to the manufacturer's recommendations. Cytokine concentration in serum was analyzed using a CytoFLEX flow cytometer and LEGENDplex software (BioLegend). As a positive control of systemic inflammation, mice were injected with 200 μg of anti-CTLA4 clone 9H10 (BioXcell) as described previously (30, 31). Lungs, livers, and small intestines were fixed in 10% formalin, and embedded in paraffin, and sectioned. Seven-micron–thick sections were stained with H&E to assess inflammation.

Statistical analysis

When the variables studied were normally distributed, multiple comparisons were performed using one-way ANOVA with Tukey or Dunnett posttest, and comparisons between two groups were performed using Student unpaired *t* test. Nonparametrical methods were applied for nonnormally distributed variables. For these statistical analyses, multiple comparisons were performed using Kruskall–Wallis with Dunn posttest, and comparisons between two groups were performed using Mann–Whitney *U* test. Significance of overall survival was determined via Kaplan–Meier analysis with log-rank analysis. Unsupervised clustering was performed using agglomerative hierarchical clustering with complete linkage. Heatmaps were plotted based on maximum distance measure. Hierarchical clustering was conducted using statistical software R (www.r-project.org). All statistical analyses were performed with Graphpad Prism 6 and 7 (GraphPad). Error bars show SEM, and $P < 0.05$ was considered statistically significant. * indicates $P < 0.05$, **, $P < 0.01$, ***, $P < 0.001$,

and ****, $P < 0.0001$ unless otherwise indicated. ns denotes not significant.

Results

Vaccination of tumor-bearing mice against TAP TEIPP inhibits tumor growth

Short CpG containing ODNs can serve as agonists for TLR9, and studies have shown that systemically administered siRNAs fused to a CpG ODN are preferentially taken up by TLR9-expressing DCs and B cells, activate DCs *in vitro* and *in vivo*, and downregulate the siRNA targets (24). Incubation of the murine DC cell line DC 2.4 *in vitro* with a CpG ODN conjugated to a murine TAP-specific siRNA (CpG-TAP siRNA) led to the downregulation of TAP mRNA (**Fig. 1A**), maturation of DCs (Supplementary Fig. S1A), and presentation of a previously described TAP TEIPP named TRH4 (13) to cognate T cells (**Fig. 1B**). Systemic administration of CpG-TAP siRNA to mice via subcutaneous injection led to the reduction of TAP mRNA

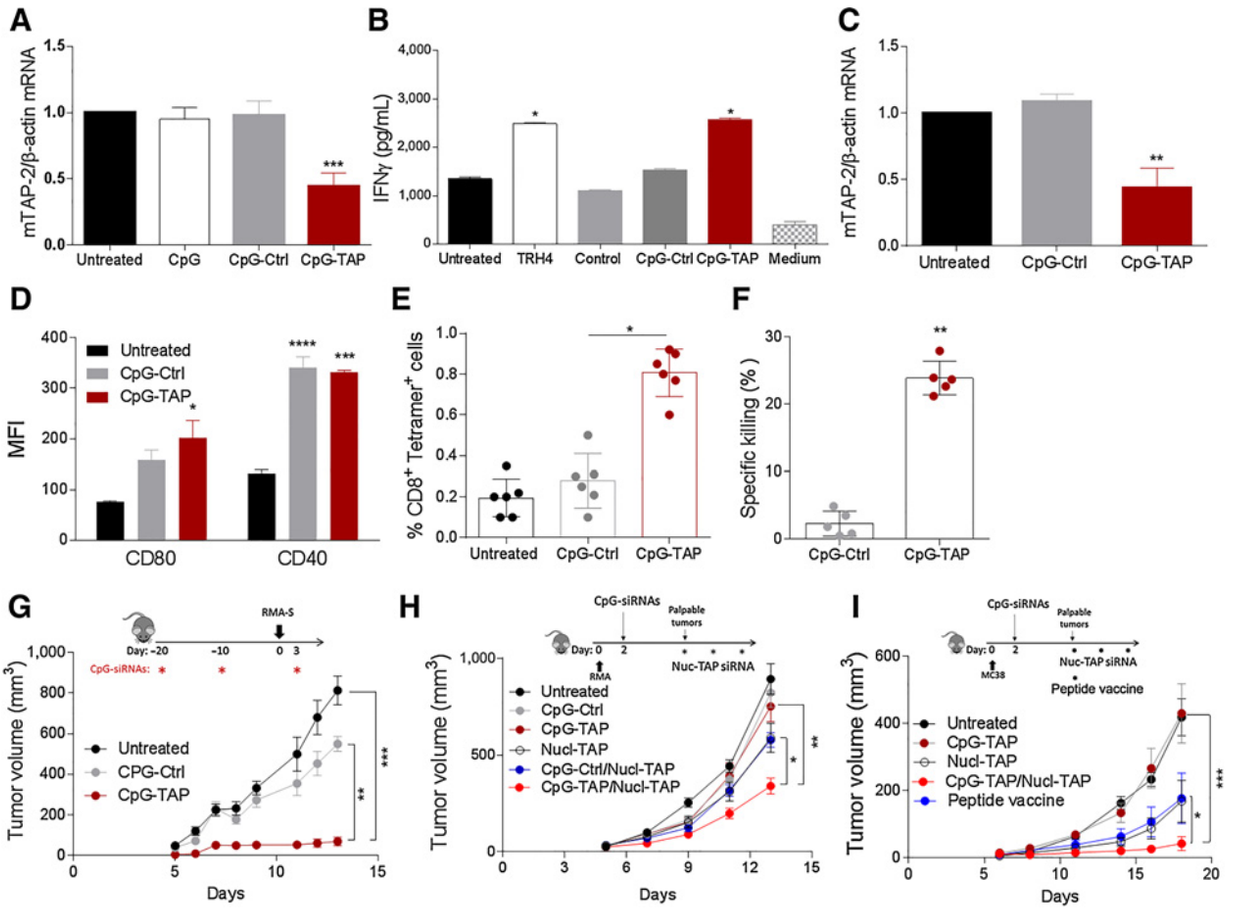

Figure 1.

Vaccination with CpG-TAP siRNA elicits T-cell responses and inhibits tumor growth in mice compared with vaccination against mutation-derived neoantigens. **A,** *Tap2* mRNA in DC2.4 cells were incubated with CpG-TAP siRNA. Cells were treated with CpG or CpG-siRNAs, and 24 hours later, RNA was isolated and quantified by qRT-PCR. Shown are means + SEM performed in triplicates ($n = 2$). **B,** DC2.4 cells were treated with CpG-siRNAs or pulsed with the TRH4 or control Ad10 peptides, and cultured with LnB5 T cells that recognize the TRH4 peptide presented by H-2b molecules (13). INFγ production after 20 hours was measured by ELISA. Shown are means + SEM of triplicate wells ($n = 2$). **C** and **D,** *Tap* mRNA expression and mean fluorescent intensity (MFI) of maturation markers in DCs *in vivo*. Mice were injected once subcutaneously with CpG-siRNAs close to inguinal lymph nodes in the right flank. Right inguinal lymph nodes were excised 24 hours later, and $CD11c^+$ cells were isolated using magnetic beads. **C,** *Tap2* mRNA was quantified by qRT-PCR using cells pooled from 2 mice (8 mice/group; $n = 2$). **D,** Expression of maturation markers in $CD11c^+$ cells was analyzed by flow cytometry. Shown are means + SEM. **E** and **F,** TAP-deficient RMA-S T lymphoma tumor–bearing mice were treated with CpG-TAP, and TRH4-specific $CD8^+$ T-cell responses were assessed. Results from two independent experiments were combined (2–3 mice/group). **E,** Staining with TRH4 tetramer on tumor-infiltrating lymphocytes 7 days after the second CpG-TAP dose administration (6 mice/group; $n = 2$). **F,** *In vivo* killing of TRH4 peptide–pulsed splenocytes, as described in Materials and Methods (5 mice/group; $n = 2$). Shown are means ± SEM. **G,** RMA-S tumor–bearing mice were vaccinated with CpG-TAP following the indicated regimen, and tumor growth was assessed. Shown are means ± SEM for tumor volumes (7 mice/group; $n = 3$). **H,** RMA T lymphoma tumor–bearing mice were treated with CpG-TAP and Nucl-TAP siRNAs following the indicated regimen. Shown are mean ± SEM for tumor volumes (7–9 mice/group; $n = 2$). **I,** MC38 tumor–bearing mice were treated with CpG-TAP and Nucl-TAP siRNAs following the indicated regimen and compared to mice vaccinated against tumor-resident neoantigens. Data show mean ± SEM for tumor volumes. Results from two independent experiments were combined (11–14 mice/group). **A–D,** Statistical analyses using one-way ANOVA test and Dunnet posttest for comparisons between untreated and all conditions. **E,** Statistical analysis using one-way ANOVA test and Tukey posttest. **F,** Statistical analyses using Mann-Whitney *U* test. **G–I,** Statistical analyses using Kruskal–Wallis test and Dunn posttest. Differences are indicated in the graphs: *, $P < 0.05$; **, $P < 0.01$; ***, $P < 0.001$; and ****, $P < 0.0001$.

expression in lymph node DCs (**Fig. 1C**), *in situ* maturation of DCs (**Fig. 1D**), and induction of a T-cell response against the TRH4 epitope measured by tetramer staining (**Fig. 1E**) and an *in vivo* cytotoxic assay (**Fig. 1F**). Taken together, these experiments showed that a CpG ODN could target a TAP siRNA to DCs *in vitro* and *in vivo*, leading to the downregulation of TAP and presentation of MHC class I–restricted epitopes.

To determine whether the CpG-TAP siRNA-induced immune response can inhibit the growth of tumor cells with reduced TAP expression, CpG-TAP siRNA–treated mice were challenged with TAP-deficient RMA-S tumor cells. Tumor growth was significantly inhibited when mice were treated with CpG-TAP, but not with CpG-Ctrl, siRNA (**Fig. 1G**). We previously showed that administration of a TAP-specific siRNA conjugated to a broad-range tumor-targeting nucleolin aptamer (Nucl-TAP siRNA) leads to a partial downregulation of TAP in tumor cells, presentation of TAP TEIPP in murine and human cells, and inhibits tumor growth in multiple tumor models (23). Here, we tested whether vaccination against TAP TEIPP would enhance the antitumor immune response elicited by said antigens induced in the tumor cells. Vaccination of TAP-sufficient RMA tumor–bearing mice with CpG-TAP siRNA enhanced the effect of Nucl-TAP siRNA, whereas vaccination with CpG-TAP siRNA alone or vaccination with CpG-Ctrl siRNA and Nucl-TAP siRNA had no (additive) effects (**Fig. 1H**).

Tumor-resident mutation-generated neoantigens are thought to be the most effective antigenic targets for vaccination. We, therefore, compared the potency of vaccination against TAP TEIPP induced in the developing tumor to vaccination against a mixture of three prototypic mutation-derived neoantigens expressed in MC38 adenocarcinoma tumors (29). The MC38-resident neoantigens have been identified by sequential exome sequencing, characterization of MHC class I-associated peptides by mass spectrometry, and their ability to elicit T-cell responses in mice (29). Whereas vaccination of MC38 tumor–bearing mice with a mixture of the three neoantigens exhibited a small but discernible inhibitory effect on the growth of MC38 tumors as described previously (29) and was comparable to inducing TAP TEIPP in the tumor cells by treatment with Nucl-TAP siRNA (23), vaccination with CpG-TAP siRNA followed by treatment with Nucl-TAP siRNA was significantly more effective (**Fig. 1I**). Tumor volumes showed that the magnitude of the antitumor response with the peptide mixture was comparable with what has been described (ref. 29; Supplementary Fig. S1B).

Whereas vaccination with CpG-TAP siRNA alone did not affect the growth of TAP-sufficient RMA (**Fig. 1H**), MC38 (**Fig. 1I**), or breast carcinoma 67NR tumor–bearing mice (Supplementary Fig. S1C), conceivably because they did not present TAP TEIPP, vaccination with CpG-TAP siRNA inhibited the growth of 4T1 tumors, which could be further enhanced by treatment with Nucl-TAP siRNA (Supplementary Fig. S1D). The partial susceptibility of 4T1 tumors to CpG-TAP siRNA vaccination was likely due to reduced TAP mRNA (Supplementary Fig. S1E) and MHC class I (Supplementary Fig. S1F and S1G) expression compared with the nonmetastatic variant 67NR tumor cells, which was derived from the same thioguanine-resistant tumor originating in a BALB/c mouse (32).

Vaccination against TAP TEIPP inhibits recurrent and future tumor growth

Vaccination against the experimentally induced TAP TEIPP is suitable for vaccinating against future tumors. Tumor-resident mutation-derived neoantigens may differ between the recurring tumor that develops after a long latency and the biopsy used to identify the neoantigens and prepare the vaccine, whether due to immune editing (7–10) or because metastatic lesions often originate from early disseminating tumor cells (11). For individuals at risk of developing cancer, which neoantigens will be expressed in the future tumor cannot be predicted (12). Here, we tested whether and to what extent vaccination against TAP TEIPP could inhibit the growth of recurring or future tumors, provided the said antigens would be induced when tumors develop. The two-step procedure depicted in **Fig. 2A** is composed of vaccinating against TAP TEIPP with CpG-TAP siRNA (i.e., prophylactic vaccination), followed by induction of said antigens in the developing tumor with Nucl-TAP siRNA. To test this concept, mice were vaccinated twice by subcutaneous administration of CpG-TAP siRNA before tumor challenge and a third time 2 days after subcutaneous tumor inoculation. Although both vaccination before or after RMA-S tumor challenge inhibited tumor growth, the combination was significantly more effective (Supplementary Fig. S2A). Vaccination of RMA tumor–bearing C57BL/6 (H-2b) mice with CpG-TAP siRNA led to pronounced inhibition of tumor growth, provided the mice were also treated with Nucl-TAP, but not Nucl-Ctrl, siRNA (**Fig. 2B**). Vaccination against the TAP TEIPP was less effective against 4T1 tumor–bearing BALB/c (H-2d) mice, and as seen before (Supplementary Fig. S1D), CpG-TAP siRNA vaccination alone also inhibited tumor growth, conceivably due to the reduced expression of TAP mRNA in the tumor cells (Supplementary Fig. S1E–S1G). Similarly, vaccination against ER aminopeptidase-associated with antigen processing (ERAAP), another key mediator of MHC class I processing whose dysfunction is shown to induce the presentation of novel MHC class I–restricted epitopes (33), inhibited the growth of subsequently implanted RMA tumor cells that was dependent on treatment of the tumor-bearing mice with Nucl-ERAAP siRNA (Supplementary Fig. S2B).

We next evaluated the vaccination protocol in autochthonous models of recurrence and premalignant disease. We used a model of recurrence whereby pancreatic KPC-derived tumor cells mixed with stellate cells were implanted orthotopically into the pancreas (26), and tumors were resected when they become palpable (**Fig. 2C**). Resection alone had a small survival benefit that was not improved by CpG-TAP vaccination. Whereas Nucl-TAP siRNA treatment exhibited a small therapeutic benefit resulting from the induced expression of the TAP TEIPP in the residual tumor cells, consistent with our previous study (23), combination of CpG-TAP vaccination followed by Nucl-TAP treatment led to a significant enhancement of survival. To evaluate the vaccination protocol against future tumors, we used the MCA carcinogen-induced model for fibrosarcoma (ref. 34; **Fig. 2D**) and the PyV-MT model for breast cancer (ref. 35; **Fig. 2E**, Supplementary Fig. S2D), whereby mice were vaccinated in the premalignant stage and antigen induced when tumors became palpable. In both models, combination of CpG-TAP siRNA vaccination and Nucl-TAP siRNA antigen induction led to a significant enhancement of survival. In the MCA model, tumors regressed in a significant proportion of the treated mice (Supplementary Fig. S2C). Taken together, these experiments showed that (i) vaccination against TAP TEIPP could inhibit future tumor growth, provided said antigens were induced by targeted inhibition of TAP in the developing tumors; (ii) vaccination against the experimentally induced TAP TEIPP was not dependent on prior knowledge of the antigenic content of concurrent, recurring, or future tumors; and (iii) the TAP TEIPP was prototypic of a class of antigens induced by downregulation of key mediators of antigen processing, such as ERAAP (Supplementary Fig. S2B).

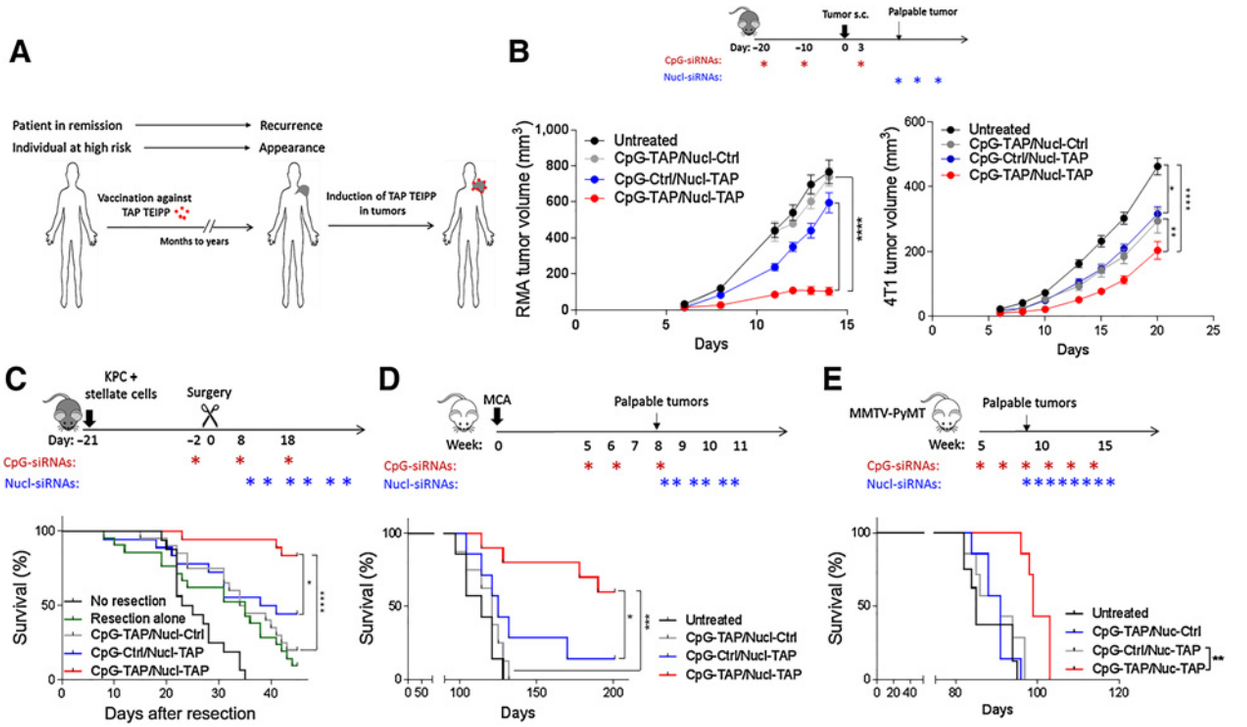

Figure 2.

Vaccination against TAP downregulation–induced antigens inhibits the growth of future tumors. **A,** Vaccination against antigens induced in future tumors for patients in remission or individuals at high risk of developing cancer. Patients in remission are vaccinated against TAP TEIPP, and when tumors will inevitably recur, (the same) antigens are induced in the developing tumor. Individuals at high risk of developing cancer are vaccinated against TAP deficiency-induced antigens and if or when tumors develop, the (same) antigens are induced in the developing tumor. **B,** Mice were vaccinated with CpG-siRNA, implanted subcutaneously with RMA (left) or 4T1 (right) tumor cells, and treated with Nucl-siRNA as indicated. Shown are means ± SEM for tumor volumes (7–8 mice/group, $n = 2$). **C,** A mixture of KPC-derived tumor cells and stellate cells was surgically implanted into the pancreas of mice. When tumors became palpable, they were resected, and mice were vaccinated with CpG-TAP siRNA and Nucl-TAP siRNA as indicated. Survival is shown. Results from two independent experiments were combined (8–12 mice/group). **D,** MCA-induced model for fibrosarcoma. Mice were treated with MCA, were vaccinated with CpG-TAP siRNA, and when tumors became palpable, were treated with Nucl-TAP siRNA as indicated (7–10 mice/group, $n = 1$). Survival is shown. **E,** Transgenic PyV-MT mice were vaccinated during the premalignant stage as indicated, and when tumors became palpable, antigens were induced with Nucl-TAP siRNA. Survival is shown (7–10 mice/group, $n = 1$). Statistical analyses using Kruskal–Wallis test and Dunn posttest (**B**). Survival curves analyzed by log-rank (Mantel–Cox) test (**C–E**). Differences are indicated in the graphs (*, $P < 0.05$; **, $P < 0.01$; ***, $P < 0.001$; and ****, $P < 0.0001$).

TAP TEIPP–specific T cells recognize human tumor cells with reduced TAP expression

To determine whether vaccination against TAP TEIPP could be applicable to human patients, we tested whether DCs pulsed with CpG-TAP siRNA were capable of stimulating *in vitro* $CD8^+$ T cells to recognize tumor cells treated with Nucl-TAP siRNA. We previously showed that human tumor cells treated *in vitro* with a human TAP siRNA conjugated to the nucleolin aptamer present an HLA-A2–restricted TAP TEIPP, called peptide 14 (p14; ref. 25) that is induced in TAP-deficient human tumor cells of distinct origin (23). Similarly, human monocyte-derived DCs treated with the CpG ODN conjugated to a human TAP specific siRNA led to the partial downregulation of TAP mRNA (**Fig. 3A**) and presentation of p14 to a cognate T-cell clone (**Fig. 3B**). CpG-TAP siRNA–treated DCs stimulated autologous $CD8^+$ T cells, which recognized both TAP-deficient as well as Nucl-TAP, but not Nucl-Ctrl, siRNA-treated TAP-sufficient tumor cells (**Fig. 3C**). Cells that downregulate TAP present multiple epitopes mostly derived from housekeeping products (17). The CpG-TAP siRNA-stimulated $CD8^+$ T cells recognized DCs pulsed with HLA-A2–restricted peptides (**Fig. 3D**) that were presented by TAP-deficient tumor cells (25). This suggests that CpG-TAP siRNA-treated DCs could stimulate a polyclonal $CD8^+$ T-cell response against multiple shared TAP TEIPP also presented by TAP-deficient tumor cells, and thereby could enhance the recognition of a broad range of tumors with reduced TAP expression.

In progressing human tumors TAP is often downregulated in a proportion of tumor cells that is more prevalent in metastatic lesions (36–39), and reviewed in ref. 40. Analysis of a pair of non-metastatic SW480 and metastatic SW620 cell lines established from a patient with colon cancer showed that the metastatic variant expressed lower TAP mRNA (Supplementary Fig. S3A), presented the p14 TAP TEIPP to a cognate $CD8^+$ T-cell clone measured by cell killing (Supplementary Fig. S3B) or IFNγ secretion (Supplementary Fig. S3C), and $CD8^+$ T cells stimulated with CpG-TAP–treated autologous DCs recognized metastatic SW620, but not nonmetastatic SW480, tumor cells (Supplementary Fig. S3D). The susceptibility of metastatic 4T1, but not the nonmetastatic 67NR, tumor variant to CpG-TAP vaccination in mice (Supplementary Fig. S1C–S1G) and the presentation of TAP TEIPP by the human metastatic colorectal cancer variant (Supplementary Fig. S3) raises the possibility that metastatic lesions harboring a significant proportion of cells with reduced TAP expression could be susceptible to CpG-TAP siRNA vaccination, even in the absence of Nucl-TAP siRNA treatment. Given, however, the

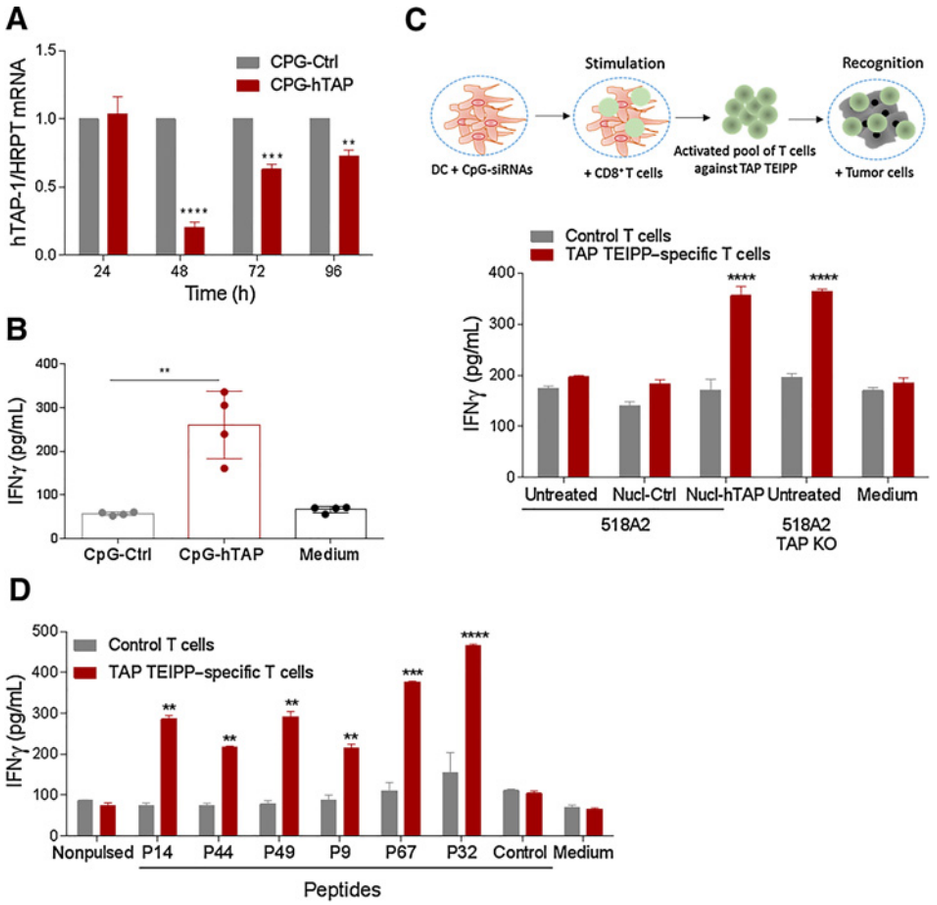

Figure 3.

CpG-TAP siRNA-pulsed DCs stimulate human PBMC-derived CD8$^+$ T cells *in vitro*, which recognize tumor cells with reduced TAP expression. **A,** Human *TAP1* mRNA expression in DCs treated with CpG-TAP siRNA. Monocyte-derived human DCs were treated with CpG-Ctrl or TAP siRNAs, and at indicated time points, mRNA was generated and quantified by qRT-PCR. Shown are means + SEM performed in duplicates. Results from two independent experiments were combined. **B,** Presentation of p14, a TAP deficiency–induced peptide, in 518A2 melanoma cells treated with Nucl-siRNAs and cultured with a cognate CD8$^+$ T-cell clone that recognized the HLA-A2–p14 complex (25). IFNγ production after 20 hours was measured by ELISA. Means ± SEM of quadruplicate wells ($n = 2$). **C,** Stimulation of TAP TEIPP–specific CD8$^+$ T cells. CD8$^+$ T cells from an HLA-A2 donor were stimulated with autologous DCs treated with CpG-TAP siRNA. After two rounds of stimulation, CD8$^+$ T cells were isolated and cocultured with TAP-deficient 518A2 cells (518A2 TAP KO) or with TAP-sufficient parental cells (518A2) treated with Nucl-siRNAs. IFNγ production after 20 hours was measured by ELISA. Shown are means + SEM of quadruplicate wells ($n = 2$). **D,** Polyclonality of the TAP TEIPP–specific CD8$^+$ T cells. CD8$^+$ T-cell cultures, as described in **C**, were incubated with 518A2 cells pulsed with six previously described HLA-A2–restricted TAP deficiency–induced peptides (25). MAGE peptide was used as negative control. INFγ production after 20 hours was measured by ELISA. Shown are means + SEM of quadruplicate wells ($n = 2$). Statistical analyses using Student unpaired *t* test (**A**, **C**, and **D**). Statistical analyses using Kruskal–Wallis test and Dunn posttest (**B**). Differences are indicated in the graphs (**, $P < 0.01$; ***, $P < 0.001$; and ****, $P < 0.0001$).

extensive variability of TAP downregulation in human tumor lesions, which is hard to model in murine studies, only clinical trials will be able to determine whether this will be the case.

Adaptive and innate immune responses elicited by vaccination with CpG-TAP siRNA

We next evaluated the immunologic mechanism underpinning the antitumor effect of vaccinating against TAP TEIPP using the subcutaneous 4T1 tumor model. In this model, treatment with either Nucl-TAP or CpG-TAP siRNAs inhibited tumor growth (**Fig. 2B**), the latter because in 4T1 TAP expression is partially downregulated (Supplementary Fig. S1E), whereas combined treatment with CpG-TAP and Nucl-TAP siRNA led to an enhanced antitumor response (**Fig. 2B**). Inhibition of tumor growth correlated with a pronounced proinflammatory response at the tumor site in mice treated with both CpG-TAP and Nucl-TAP siRNAs, an increase in CD8$^+$ and CD4$^+$ T cells, cross-presenting CD103$^+$ DCs, M2 to M1 polarization of macrophages, a decrease in CD4$^+$ regulatory T cells (Treg) and granulocytic myeloid-derived suppressor cells (MDSC), as well as an increase in the ratio of CD8$^+$ cells to myeloid cells, Tregs, and granulocytic MDSCs (**Fig. 4A**; Supplementary Fig. S4). The proinflammatory response was less pronounced in mice treated with Nucl-TAP siRNA, and minimal in mice treated with CpG-TAP siRNA.

Tumor inhibition of subcutaneously implanted 4T1 tumor–bearing mice treated with CpG-TAP and Nucl-TAP siRNAs (**Fig. 2B**) was dependent on CD8$^+$, but not on CD4$^+$ or NK, cells (**Fig. 4B**), and adoptive transfer of CD8$^+$ T cells from naïve mice treated with CpG-TAP inhibited the growth of TAP-deficient RMA-S

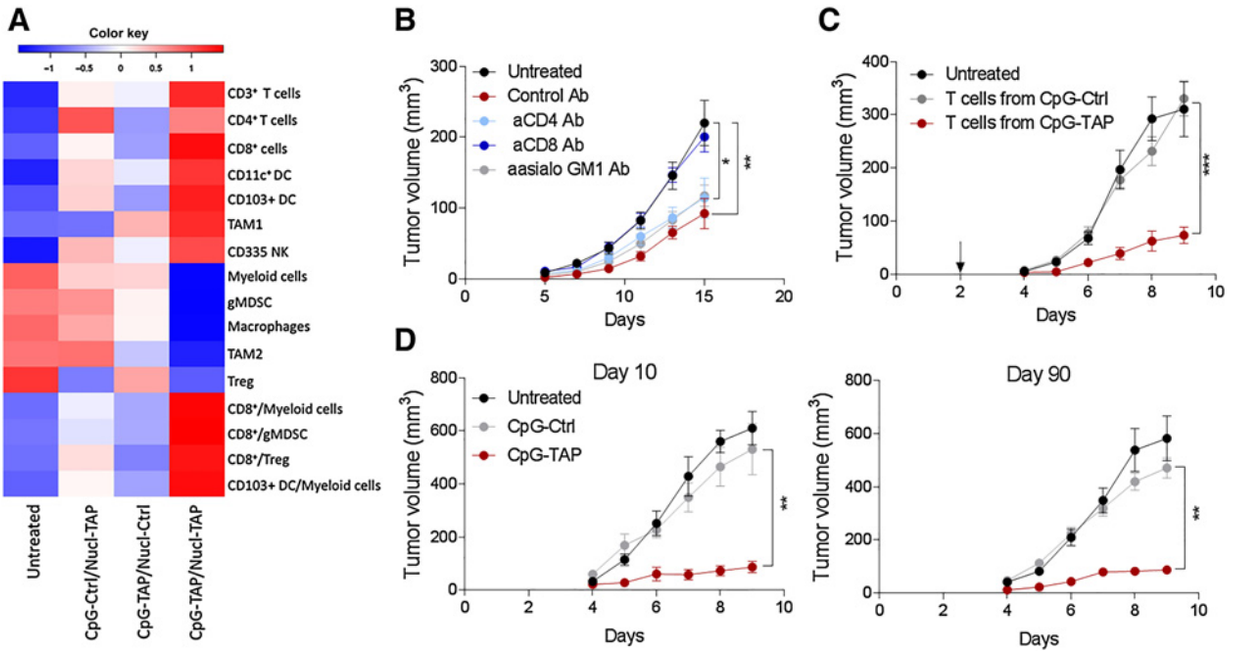

Figure 4.

Immunologic mechanism of vaccinating against TAP TEIPP. **A,** Vaccination in the 4T1 model with CpG-TAP and Nucl-TAP siRNAs as shown in **Fig. 2B**. Tumors were excised 2 days after the second Nucl-TAP siRNA treatment, and cell suspensions were generated and analyzed by flow cytometry. Shown is unsupervised clustering of immune subsets among $CD45^+$ cells (5 mice/group, $n = 2$). See gating strategy and immune subset percentages in Supplementary Fig. S4A and S4B. gMDSC, granulocytic myeloid-derived suppressor cell. **B,** Mice were vaccinated with CpG-TAP siRNA, challenged subcutaneously with 4T1 tumor cells, and treated with Nucl-TAP siRNA as described in **Fig. 2B**. Cellular subsets were depleted with antibodies (Ab) once weekly starting 3 days before the first CpG-TAP administration. Shown are means ± SEM for tumor volumes (7–8 mice/group, $n = 2$). **C,** RMA-S–bearing mice received one infusion of $CD8^+$ T cells (0.25×10^6) 2 days after tumor implantation as indicated by arrow. Naïve mice were vaccinated with CpG-siRNAs three times 10 days apart, and $CD8^+$ T cells were isolated 5 days after the third vaccination. Shown are mean and SEM tumor volume measurements (7–8 mice/group, $n = 1$). **D,** Mice were vaccinated with CpG-siRNAs twice 10 days apart and challenged with TAP deficient RMA-S cells 10 or 90 days after the second vaccination. A third vaccination with CpG-TAP siRNA was administered 3 days after tumor implantation to all mice. Shown are means ± SEM for tumor volumes (5–10 mice/group, $n = 1$). Statistical analyses using Kruskal–Wallis test and Dunn posttest (**B–D**). Differences are indicated in the graphs (*, $P < 0.05$; **, $P < 0.01$; and ***, $P < 0.001$).

tumors (**Fig. 4C**). Vaccination of mice with CpG-TAP siRNA engendered long-lasting protective immunity. No diminution of tumor inhibition was seen when vaccinated mice were challenged with TAP-deficient tumor cells 90 days following vaccination compared to 10 days following vaccination (**Fig. 4D**). Consistent with this, 30 days following treatment with CpG-TAP, but not CpG-Ctrl, siRNA, about 1% of total $CD44^+KLRG^-$ memory and $CD62L^+KLRG^-$ central memory $CD8^+$ T cells in the spleen or draining lymph nodes were specific to TRH4 TAP TEIPP (Supplementary Fig. S5). Given that TAP downregulation induces the presentation of multiple epitopes (17, 25), the proportion of vaccine-induced TAP TEIPP was likely significantly higher.

Vaccination against TAP TEIPP does not elicit autoimmunity

In clinical trials, CpG ODNs used as immune adjuvants (41) and the nucleolin aptamer used as a cytotoxic agent (42), were administered at 10–100 fold higher doses than used in our studies as targeting agents (prorated for weight). Both CpG ODNs and the nucleolin aptamer were well tolerated and did not elicit significant toxicities in patients. Yet, given that TAP TEIPP are encoded in housekeeping products that are not presented under normal conditions (17), autoimmunity could develop if the otherwise cryptic epitopes are presented to the CpG-TAP siRNA vaccination-induced T cells by normal cells that have downregulated TAP, or despite tumor targeting by nucleolin aptamer, some of the siRNA could be taken up by normal cells. We did not see evidence of toxicity in mice vaccinated against TAP TEIPP in terms of morbidity, complete blood counts (Supplementary Table S1), elevated cytokines in circulation (Supplementary Fig. S6A), liver damage measured by circulating liver enzymes alanine transaminase (ALT) and aspartate transaminase (AST; **Fig. 5A**), or nonspecific inflammation in the liver, small intestine, or lungs (**Fig. 5B**; Supplementary Fig. S6B). In contrast, mice treated with a comparable therapeutic dose of CTLA-4 antibody elicited organ-wide inflammatory responses similar to the toxicities often seen in human patients (refs. 30, 31; indicated by the arrows in **Fig. 5B**). Taken together, our studies suggest that vaccinating against TAP TEIPP could be safe or less toxic than treatment with CTLA-4 antibodies.

Dispensing with the need for inducing TAP TEIPP in tumor cells

The vaccination protocol as described above is a two-step, two-reagent protocol (**Fig. 2A**) using vaccination against induced antigens with CpG-TAP siRNA and inducing said antigens in the tumor with Nucl-TAP siRNA. There are, however, two scenarios encompassing a significant proportion of cancers, B-cell malignancies and human papillomavirus (HPV)–induced cancers, where the second step of inducing antigens with Nucl-TAP siRNA could be omitted. Most B-cell–derived tumors also express TLR9, the endocytic receptor of

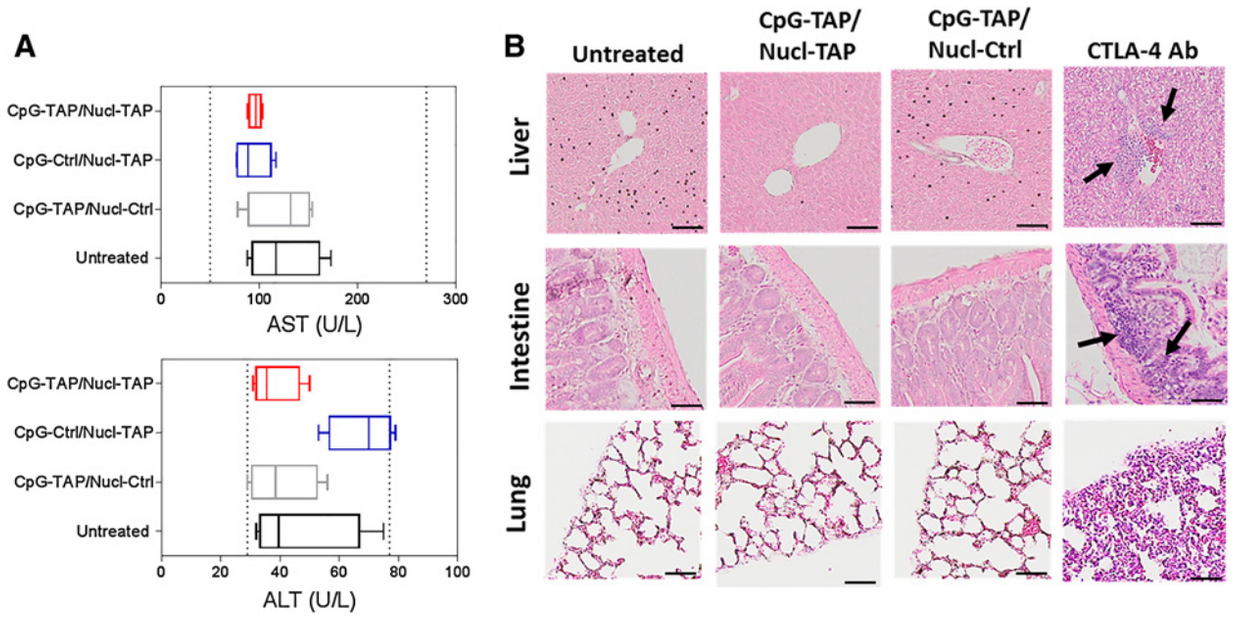

Figure 5.

Toxicity of vaccinating against TAP TEIPP. Naïve mice (4 mice/group) were administered CpG-siRNAs and Nucl-siRNAs as described in **Fig. 2B** but without tumor implantation. **A,** Liver pathology. ALT and AST levels in the circulation measured by ELISA. Bracketed area represents normal levels of ALT or AST in BALB/c mice [from The Jackson Laboratories (Mouse Phenome Database, http://phenome.jax.org/)]. Data represent box plot analysis (min to max). **B,** Inflammatory responses in tissue sections stained with hematoxylin and eosin and visualized by light microscopy at 40× magnification (scale bar, 25 μm). One group of mice was treated with 200 μg of CTLA-4 antibody (Ab) that elicits a comparable antitumor effect. Arrows indicate inflammatory foci in mice.

CpG ODN. Hence, the CpG-TAP siRNA could be used both for vaccination and for antigen induction in B-cell tumors. In support of this hypothesis, a single administration of CpG-TAP siRNA to TLR9-expressing A20 B lymphoma tumor-bearing mice inhibited tumor growth that could not be attributed to the adjuvant effect of CpG ODNs (**Fig. 6A**). Previous studies have shown that targeted inhibition of STAT3, a broad-spectrum mediator of immune suppression, using an siRNA or DNA decoy conjugated to a CpG ODN, inhibited the growth of B-cell lymphoma in mice (27, 28). Underscoring the importance of potentiating vaccine-induced antitumor immunity using experimental conditions, whereby CpG-TAP siRNA or CpG-STAT3 DNA decoy exhibit a limited impact, combining CpG-TAP siRNA treatment with CpG-STAT3 DNA decoy significantly reduced tumor growth (Supplementary Fig. S7) and enhanced the survival of the treated mice (**Fig. 6B**). Consistent with the ability of CpG-TAP siRNA to both induce T-cell responses and express TAP TEIPP on B-cell–derived tumor cells, incubation of CpG-TAP siRNA with human B cell-derived tumor cell lines Ramos or TMD8 downregulated TAP mRNA (**Fig. 6C**) and presented the p14 TAP TEIPP to a cognate T-cell clone measured as killing of the tumor cells (**Fig. 6D**) or IFNγ secretion from the T cells (**Fig. 6E**). $CD8^+$ T cells stimulated with CpG-TAP, but not CpG-Ctrl, siRNA-treated DCs recognized Ramos and TMD8 cells (**Fig. 6F**), provided the tumor cells were treated with CpG-TAP siRNA.

Culture-established HPV-transformed cells express reduced TAP activity (43, 44), raising the possibility that vaccination with CpG-TAP siRNA as single agent may be also effective against HPV-induced tumors. Consistent with this hypothesis, murine HPV^+ TC-1 tumor cells presented the TRH4 TAP TEIPP in culture (**Fig. 6G**), and vaccination of TC-1 tumor–bearing mice with CpG-TAP siRNA inhibited tumor growth (**Fig. 6H**). Human cervical HPV^+ Caski, but not the HPV^- C33A, cancer cells presented p14 TAP TEIPP (**Fig. 6I**), and CpG-TAP–stimulated $CD8^+$ T cells recognized HPV^+ Caski, but not the HPV^-, C33A cells (**Fig. 6J**). It, however, remains to be seen whether and to what extent TAP is downregulated in HPV^+ tumors *in vivo*.

Discussion

Here, we describe a vaccination strategy against experimentally induced antigens that target tumor cells "marked" for recognition by a vaccine-elicited immune response. We showed that vaccination against antigens induced by downregulating TAP (TAP TEIPP) in TLR9-expressing professional antigen-presenting cells with CpG-TAP siRNA is potent, broadly applicable, and safe, provided TAP is also downregulated in tumor cells with Nucl-TAP siRNA.

Two sets of observations suggest that vaccinating against TAP TEIPP is potent. First, it was more effective than vaccination against mutation-derived neoantigens expressed in the MC38 tumor. This comparison may underestimate the effectiveness of vaccinating against TAP TEIPP because the MC38-expressed neoantigens were clonal in nature and hence therapeutically the most potent neoantigens, yet the identification of the rare clonal neoantigens in human tumors will be particularly challenging (1, 2). Second, using stringent and increasingly informative autochthonous models of recurrence and premalignant disease, we showed that vaccination against TAP TEIPP cleared tumors in a proportion of mice in a recurrence model for pancreatic cancer and a premalignant model for carcinogen-induced fibrosarcoma and delayed tumor development in the challenging PyV-MT model for breast cancer. Arguably, the modest effect seen in the PyV-MT model is more likely to represent what we can expect to achieve under best circumstances in human patients

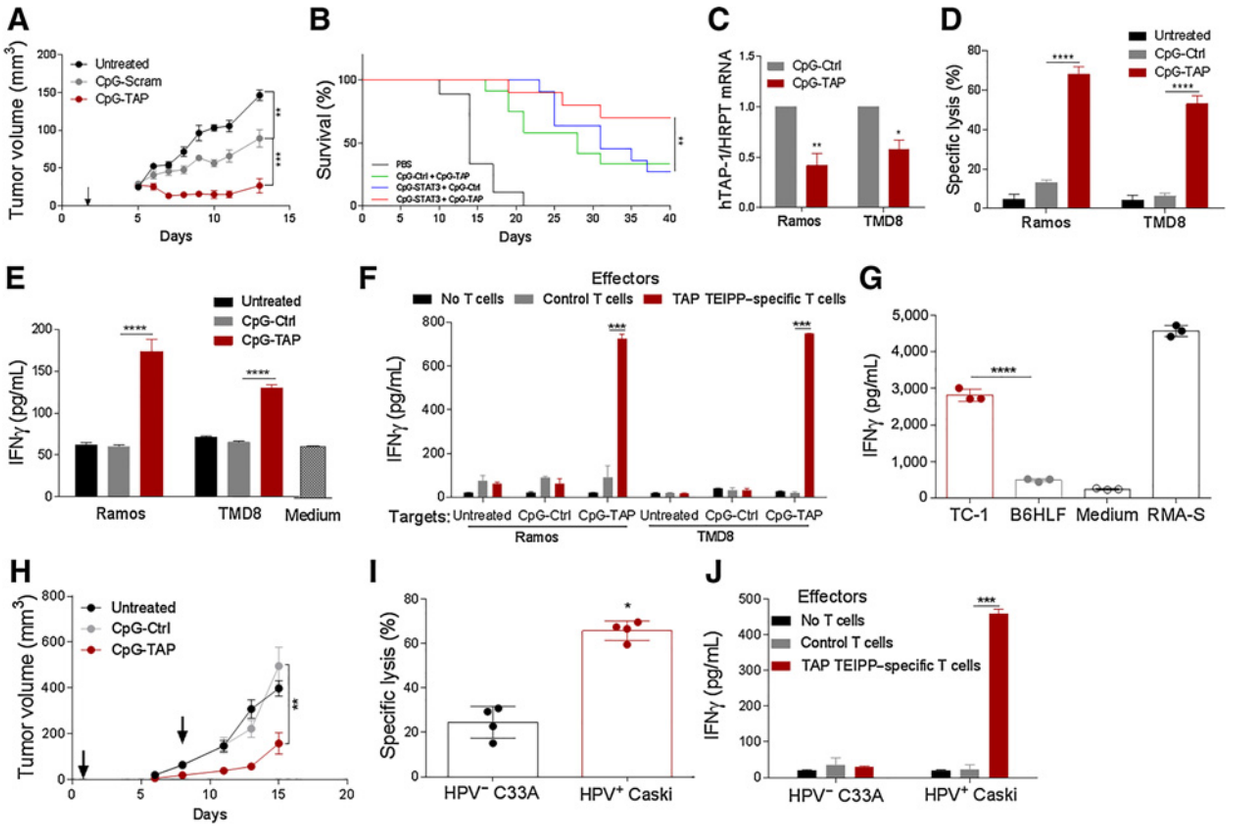

Figure 6.

CpG-TAP siRNA vaccination against TAP TEIPP does not require Nucl-TAP siRNA antigen induction in B-cell malignancies and HPV-induced cancers. **A–F,** B-cell tumors. **A,** Subcutaneously implanted A20 tumor–bearing mice received one injection of CpG-Ctrl or CpG-TAP siRNA 2 days after tumor implantation as indicated by arrow. Shown are means ± SEM for tumor volumes (7 mice/group, $n = 2$). **B,** BALB/c mice were injected i.v. (tail vein) with 5×10^6 A20 cells expressing luciferase ($A20^{Luc}$), and tumor growth was monitored as described previously (27, 28). After 9 days, mice were treated with 1 mg/kg CpG-TAP siRNA (CpG-TAP) twice on day 1 and day 7 after treatment and then with 5 mg/kg CpG-STAT3 DNA decoy (CpG-STAT3dODN) every other day for a total of eight injections. Survival of the treated mice is shown. Results are combined from two independent experiments (CpG-STAT3dODN + CpG-siTAP group: $n = 10$; CpG-STAT3dODN + CpG-SCR group: $n = 11$; CpG-SCR + CpG-siTAP group: $n = 11$; PBS group: $n = 9$; ****, $P < 0.0001$). **C,** Human *TAP1* mRNA in RAMOS and TMD8 B-lymphoma cells incubated with CpG-TAP. Cells were treated with CpG-siRNAs, and 48 hours later, RNA was isolated and quantified by qRT-PCR. Shown are means + SEM performed in duplicates. Results from four independent experiments were combined. **D** and **E,** Cells were treated with CpG-siRNAs for 72 hours and cultured with a $CD8^+$ T-cell clone that recognized the HLA-A2–restricted p14 complex (25). **D,** *In vitro* cytotoxicity of the tumor cells after 4 hours coculture was determine by lactate dehydrogenase assay. Shown are means + SEM. **E,** IFNγ production by the T-cell clone was measured by ELISA. Shown are means + SEM of quadruplicate wells ($n = 2$). **F,** $CD8^+$ T cells cocultured with CpG-TAP or CpG-Ctrl siRNA–treated autologous DCs, as described in **Fig. 3C**, were incubated with RAMOS or TMD8 cells treated with CpG-TAP or CpG-Ctrl siRNA. IFNγ production was measured after a 20-hour coculture by ELISA. Shown are means + SEM of quadruplicate wells ($n = 2$). **G–J,** HPV^+ tumors. **G,** HPV^+ TC-1 and HPV^- B6 HLF cells were cocultured with LnB5 T cells. IFNγ production after 20 hours was measured by ELISA. RMA-S cells were used as positive control of LnB5 T-cell stimulation. Shown are means ± SEM of triplicate wells ($n = 2$). **H,** C57BL/6 mice were injected subcutaneously with TC-1 tumor cells. One and 7 days later (arrows), mice were injected with CpG-siRNAs. Shown are means ± SEM for tumor volumes (9–10 mice/group, $n = 1$). **I,** Human HPV^+ Caski cells were cocultured with a $CD8^+$ T-cell clone that recognized the HLA-A2–p14 complex. *In vitro* cytotoxicity of the tumor cells after 4 hours of coculture was determined by lactate dehydrogenase assay. Means ± SEM of quadruplicate wells ($n = 2$). **J,** A TAP deficiency epitope–enriched $CD8^+$ T polyclonal repertoire was generated as in **Fig. 3C**. IFNγ production after 20 hours was measured by ELISA. Means + SEM of quadruplicate wells ($n = 1$). Statistical analyses using Kruskal–Wallis test and Dunn posttest (**A** and **H**). Survival curves analyzed by log-rank (Mantel–Cox) test (**B**). Statistical analyses using Student unpaired *t* test (**C**). Statistical analyses using one-way ANOVA test and Dunnet posttest (**D–F** and **J**). Statistical analyses using Mann–Whitney *U* test (**I**). Differences are indicated in the graphs (*, $P < 0.05$; **, $P < 0.01$; ***, $P < 0.001$; and ****, $P < 0.0001$).

using vaccination as monotherapy, underscoring the need for a multipronged approach of complementary immune-potentiating treatments like checkpoint blockade therapy. To the best of our knowledge, vaccination against tumor resident neoantigens has not been evaluated in such autochthonous models.

The broad applicability of vaccinating against TAP TEIPP is suggested by the observations that treatment with CpG-TAP siRNA and Nucl-TAP siRNA inhibited tumor growth in mice bearing tumors of distinct origin and genetic background. We previously showed that the nucleolin aptamer can deliver TAP siRNA to tumor cells of distinct origin (23). Thus, vaccination against TAP TEIPP could be potentially applicable to virtually all patients with cancer. The nucleolin aptamer targets a broad range of human tumor cells and is well tolerated in patients with cancer, but its tumor specificity was not conclusively demonstrated (42). Thus, the nucleolin-binding aptamer used in these proof-of-concept studies should be viewed as a prototype of tumor-targeting ligands, but its utility as tumor-targeting ligand in human patients remains to be determined. Examples of alternative targets are EpCAM exposed for ligand

recognition on carcinomas, PSMA expressed on prostate cancer, or Her2 expressed on a proportion of breast cancers.

Given that TAP TEIPP are cryptic epitopes encoded in normal products, treatment with CpG-TAP and Nucl-TAP siRNA runs the risk of eliciting autoimmune pathology. Our studies in mice failed to uncover any adverse effects or signs of autoimmunity, in stark contrast to treatment with CTLA-4 antibody that elicited organ-wide inflammatory responses similar to what is often seen in patients treated with ipilimumab (31, 45, 46). Thus, vaccination against TAP TEIPP experimentally induced in tumor cells appears to be safe, exhibiting a therapeutic index superior to that of checkpoint blockade with CTLA-4 antibody. Despite the inherent limitations of preclinical murine models to assess toxicity in human patients, it is noteworthy that murine studies have predicted both the pattern and relative intensity of adverse effects accompanying checkpoint blockade with PD-1 and CTLA-4 antibodies (31, 45, 46).

Vaccinating against TAP TEIPP offers potentially significant advantages over vaccination against tumor-resident mutation-derived neoantigens: First, unlike the vast majority of mutation-derived neoantigens (3), the TAP TEIPP could be shared among all the tumor cells of the patient (17), and the systemic administration of Nucl-TAP siRNA could ensure that all the disseminated tumor lesions of the patient will present the same set of induced antigens. We previously showed that treatment of murine or human tumor cells of distinct origin with Nucl-TAP siRNA led to the presentation of a common epitope previously described in TAP-deficient tumor cells (23). TAP downregulation induces the presentation of shared antigens in DCs and tumor cells is the underlying premise of the vaccination strategy described in this study. We showed that TAP downregulation in DCs with CpG-TAP siRNA elicited an immune response that recognized human tumor cells *in vitro* and inhibited the growth of tumor cells in mice, provided TAP was also downregulated in the tumor cells with Nucl-TAP siRNA. Second, vaccinating against TAP TEIPP would be applicable to all patients with cancer, including the majority of patients that do not express, or express too few, tumor-resident mutation-derived neoantigens (1, 2). Third, vaccination against experimentally induced shared TAP TEIPP employs two chemically synthesized off-the-shelf oligonucleotides, CpG-TAP siRNA and Nucl-TAP siRNA; for B-cell malignancies and HPV-induced cancers the need to induce antigens in the tumor cells with Nucl-TAP siRNA may be omitted. In contrast, identifying mutation-derived neoantigens, especially shared clonal neoantigens, requires the use of patient-by-patient labor-intensive protocols that have yet to be perfected (1, 2). A study has shown that tumor progression is dictated by the least immune-responsive metastatic lesions, which also exhibit extensive variability of nonsynonymous mutations (47), suggesting that therapeutically useful neoantigens will have to be identified in the patients' less-responsive metastases and not in the readily accessible tumor lesions, which in practice would be rarely feasible. Last, because siRNA-mediated presentation of the induced antigens is transient, they are not expected to induce resistance, as seen in the case of tumor-resident mutation-derived neoantigens (22, 48–52).

An alternative approach to circumvent the limitations of targeting mutation-derived neoantigens is to vaccinate against normal products that are upregulated in tumor cells, termed tumor-associated antigens (TAA; ref. 12). For example, vaccination of individuals with a history of premalignant lesions that are at high risk of developing colon cancer against MUC1, an epithelial mucin that is hypomethylated and immunogenic in colorectal, breast, ovarian, lung, and pancreatic cancer, elicits anti-MUC1 immune responses that correlate with reduced immune suppression (53). Although the merits of vaccinating against TAP TEIPP induced in future tumors was suggested in our studies, it remains to be determined whether targeting TAAs or TAP TEIPP will be more feasible, effective, and less toxic.

The experiments described in this study represent proof-of-concept of a vaccination strategy against naturally or experimentally induced antigens. Future studies will aim at optimizing the induced TEIPP vaccination protocol in terms of the best targets to downregulate, TAP, ERAAP, invariant chain, or combination thereof, as well as improving tumor and DC targeting and development of combinatorial strategies with complementary treatments that potentiate the vaccine-induced immune responses.

Disclosure of Potential Conflicts of Interest

M. Kortylewski has ownership interest (including patents) in Bioscience-Oncology Pty Ltd. No potential conflicts of interests were disclosed by the other authors.

Authors' Contributions

Conception and design: G. Garrido, D.M. Da Silva, M. Kortylewski, V. Dudeja, T. van Hall, E. Gilboa

Development of methodology: G. Garrido, A. Ferrantella, Z. Zhang, V. Dudeja

Acquisition of data (provided animals, acquired and managed patients, provided facilities, etc.): G. Garrido, B. Schrand, A. Levay, A. Ferrantella, W.M. Kast, W.M. Kast, V. Dudeja

Analysis and interpretation of data (e.g., statistical analysis, biostatistics, computational analysis): G. Garrido, B. Schrand, A. Levay, A.R. Capote, A. Ferrantella, D. Kwon, M. Kortylewski, W.M. Kast, V. Dudeja

Writing, review, and/or revision of the manuscript: G. Garrido, B. Schrand, A. Levay, K.A. Marijt, D. Kwon, M. Kortylewski, W.M. Kast, V. Dudeja, T. van Hall, E. Gilboa

Administrative, technical, or material support (i.e., reporting or organizing data, constructing databases): G. Garrido, A.R. Capote, F. D'Eramo, K.A. Marijt, M. Kortylewski

Study supervision: M. Kortylewski, E. Gilboa

Acknowledgments

The authors thank Oliver Umland and Patricia Guevara for assistance with flow cytometry and sorting and Marcin Kortylewski for using CpG ODNs. The authors acknowledge support from the Sylvester Comprehensive Cancer Center and the Center for AIDS Research (CFAR) at the University of Miami Miller School of Medicine.

Research reported in this publication was supported by the Dodson Interdisciplinary Immunotherapy Institute and the Sylvester Comprehensive Cancer Center, Miller School of Medicine, University of Miami.

The costs of publication of this article were defrayed in part by the payment of page charges. This article must therefore be hereby marked *advertisement* in accordance with 18 U.S.C. Section 1734 solely to indicate this fact.

Received January 9, 2020; revised February 25, 2020; accepted April 8, 2020; published first April 15, 2020.

References

1. Lee CH, Yelensky R, Jooss K, Chan TA. Update on tumor neoantigens and their utility: why it is good to be different. Trends Immunol 2018;39:536–48.
2. Hu Z, Ott PA, Wu CJ. Towards personalized, tumour-specific, therapeutic vaccines for cancer. Nat Rev Immunol 2018;18:168–82.
3. Schumacher TN, Scheper W, Kvistborg P. Cancer neoantigens. Annu Rev Immunol 2019;37:173–200.
4. Fidler IJ, Balch CM. The biology of cancer metastasis and implications for therapy. Curr Probl Surg 1987;24:129–209.

5. Liotta LA, Kohn E. Cancer invasion and metastases. JAMA 1990;263:1123–6.
6. Sporn MB. The war on cancer. Lancet 1996;347:1377–81.
7. DuPage M, Mazumdar C, Schmidt LM, Cheung AF, Jacks T. Expression of tumour-specific antigens underlies cancer immunoediting. Nature 2012;482:405–9.
8. Matsushita H, Vesely MD, Koboldt DC, Rickert CG, Uppaluri R, Magrini VJ, et al. Cancer exome analysis reveals a T-cell-dependent mechanism of cancer immunoediting. Nature 2012;482:400–4.
9. Mittal D, Gubin MM, Schreiber RD, Smyth MJ. New insights into cancer immunoediting and its three component phases–elimination, equilibrium and escape. Curr Opin Immunol 2014;27:16–25.
10. Ward JP, Gubin MM, Schreiber RD. The role of neoantigens in naturally occurring and therapeutically induced immune responses to cancer. Adv Immunol 2016;130:25–74.
11. Ghajar CM, Bissell MJ. Metastasis: pathways of parallel progression. Nature 2016;540:528–9.
12. Finn OJ. The dawn of vaccines for cancer prevention. Nat Rev Immunol 2018;18:183–94.
13. van Hall T, Wolpert EZ, van Veelen P, Laban S, van der Veer M, Roseboom M, et al. Selective cytotoxic T-lymphocyte targeting of tumor immune escape variants. Nat Med 2006;12:417–24.
14. van Hall T, Laban S, Koppers-Lalic D, Koch J, Precup C, Asmawidjaja P, et al. The varicellovirus-encoded TAP inhibitor UL49.5 regulates the presentation of CTL epitopes by Qa-1b1. J Immunol 2007;178:657–62.
15. Chambers B, Grufman P, Fredriksson V, Andersson K, Roseboom M, Laban S, et al. Induction of protective CTL immunity against peptide transporter TAP-deficient tumors through dendritic cell vaccination. Cancer Res 2007;67:8450–5.
16. Doorduijn EM, Sluijter M, Querido BJ, Oliveira CC, Achour A, Ossendorp F, et al. TAP-independent self-peptides enhance T cell recognition of immune-escaped tumors. J Clin Invest 2016;126:784–94.
17. Marijt KA, Doorduijn EM, van Hall T. TEIPP antigens for T-cell based immunotherapy of immune-edited HLA class I(low) cancers. Mol Immunol 2019;113:43–9.
18. Oliveira CC, Querido B, Sluijter M, de Groot AF, van der Zee R, Rabelink MJ, et al. New role of signal peptide peptidase to liberate C-terminal peptides for MHC class I presentation. J Immunol 2013;191:4020–8.
19. McGranahan N, Furness AJ, Rosenthal R, Ramskov S, Lyngaa R, Saini SK, et al. Clonal neoantigens elicit T cell immunoreactivity and sensitivity to immune checkpoint blockade. Science 2016;351:1463–9.
20. Germano G, Lamba S, Rospo G, Barault L, Magri A, Maione F, et al. Inactivation of DNA repair triggers neoantigen generation and impairs tumour growth. Nature 2017;552:116–20.
21. Jimenez-Sanchez A, Memon D, Pourpe S, Veeraraghavan H, Li Y, Vargas HA, et al. Heterogeneous tumor-immune microenvironments among differentially growing metastases in an ovarian cancer patient. Cell 2017;170:927–38.
22. Riaz N, Havel JJ, Makarov V, Desrichard A, Urba WJ, Sims JS, et al. Tumor and microenvironment evolution during immunotherapy with nivolumab. Cell 2017;171:934–49.
23. Garrido G, Schrand B, Rabasa A, Levay A, D'Eramo F, Berezhnoy A, et al. Tumor-targeted silencing of the peptide transporter TAP induces potent antitumor immunity. Nat Commun 2019;10:3773.
24. Kortylewski M, Swiderski P, Herrmann A, Wang L, Kowolik C, Kujawski M, et al. In vivo delivery of siRNA to immune cells by conjugation to a TLR9 agonist enhances antitumor immune responses. Nat Biotechnol 2009;27:925–32.
25. Marijt KA, Blijleven L, Verdegaal EME, Kester MG, Kowalewski DJ, Rammensee HG, et al. Identification of non-mutated neoantigens presented by TAP-deficient tumors. J Exp Med 2018;215:2325–37.
26. Majumder K, Arora N, Modi S, Chugh R, Nomura A, Giri B, et al. A novel immunocompetent mouse model of pancreatic cancer with robust stroma: a valuable tool for preclinical evaluation of new therapies. J Gastrointest Surg 2016;20:53–65.
27. Zhang Q, Hossain DM, Nechaev S, Kozlowska A, Zhang W, Liu Y, et al. TLR9-mediated siRNA delivery for targeting of normal and malignant human hematopoietic cells in vivo. Blood 2013;121:1304–15.
28. Zhao X, Zhang Z, Moreira D, Su YL, Won H, Adamus T, et al. B cell lymphoma immunotherapy using TLR9-targeted oligonucleotide STAT3 inhibitors. Mol Ther 2018;26:695–707.
29. Yadav M, Jhunjhunwala S, Phung QT, Lupardus P, Tanguay J, Bumbaca S, et al. Predicting immunogenic tumour mutations by combining mass spectrometry and exome sequencing. Nature 2014;515:572–6.
30. Schrand B, Verma B, Levay A, Patel S, Castro I, Benaduce AP, et al. Radiation-induced enhancement of antitumor T-cell immunity by VEGF-targeted 4–1BB costimulation. Cancer Res 2017;77:1310–21.
31. Gangadhar TC, Vonderheide RH. Mitigating the toxic effects of anticancer immunotherapy. Nat Rev Clin Oncol 2015;11:91–9.
32. Heppner GH, Miller FR, Shekhar PM. Nontransgenic models of breast cancer. Breast Cancer Res 2000;2:331–4.
33. Shastri N, Nagarajan N, Lind KC, Kanaseki T. Monitoring peptide processing for MHC class I molecules in the endoplasmic reticulum. Curr Opin Immunol 2014;26:123–7.
34. DiGiovanni J. Multistage carcinogenesis in mouse skin. Pharmacol Ther 1992;54:63–128.
35. Maglione JE, Moghanaki D, Young LJ, Manner CK, Ellies LG, Joseph SO, et al. Transgenic Polyoma middle-T mice model premalignant mammary disease. Cancer Res 2001;61:8298–305.
36. Bandoh N, Ogino T, Katayama A, Takahara M, Katada A, Hayashi T, et al. HLA class I antigen and transporter associated with antigen processing downregulation in metastatic lesions of head and neck squamous cell carcinoma as a marker of poor prognosis. Oncol Rep 2010;23:933–9.
37. Kageshita T, Hirai S, Ono T, Hicklin DJ, Ferrone S. Down-regulation of HLA class I antigen-processing molecules in malignant melanoma: association with disease progression. Am J Pathol 1999;154:745–54.
38. Vitale M, Rezzani R, Rodella L, Zauli G, Grigolato P, Cadei M, et al. HLA class I antigen and transporter associated with antigen processing (TAP1 and TAP2) down-regulation in high-grade primary breast carcinoma lesions. Cancer Res 1998;58:737–42.
39. Cromme FV, van Bommel PF, Walboomers JM, Gallee MP, Stern PL, Kenemans P, et al. Differences in MHC and TAP-1 expression in cervical cancer lymph node metastases as compared with the primary tumours. Br J Cancer 1994;69:1176–81.
40. Hicklin DJ, Marincola FM, Ferrone S. HLA class I antigen downregulation in human cancers: T-cell immunotherapy revives an old story. Mol Med Today 1999;5:178–86.
41. Adamus T, Kortylewski M. The revival of CpG oligonucleotide-based cancer immunotherapies. Contemp Oncol 2018;22:56–60.
42. Bates PJ, Reyes-Reyes EM, Malik MT, Murphy EM, O'Toole MG, Trent JO. G-quadruplex oligonucleotide AS1411 as a cancer-targeting agent: uses and mechanisms. Biochim Biophys Acta 2017;1861:1414–28.
43. Cromme FV, Airey J, Heemels MT, Ploegh HL, Keating PJ, Stern PL, et al. Loss of transporter protein, encoded by the TAP-1 gene, is highly correlated with loss of HLA expression in cervical carcinomas. J Exp Med 1994;179:335–40.
44. Vambutas A, DeVoti J, Pinn W, Steinberg BM, Bonagura VR. Interaction of human papillomavirus type 11 E7 protein with TAP-1 results in the reduction of ATP-dependent peptide transport. Clin Immunol 2001;101:94–9.
45. Cousin S, Italiano A. Molecular pathways: immune checkpoint antibodies and their toxicities. Clin Cancer Res 2016;22:4550–5.
46. Young A, Quandt Z, Bluestone JA. The balancing act between cancer immunity and autoimmunity in response to immunotherapy. Cancer Immunol Res 2018;6:1445–52.
47. Angelova M, Mlecnik B, Vasaturo A, Bindea G, Fredriksen T, Lafontaine L, et al. Evolution of metastases in space and time under immune selection. Cell 2018;175:751–65.
48. Schietinger A, Philip M, Krisnawan VE, Chiu EY, Delrow JJ, Basom RS, et al. Tumor-specific T cell dysfunction is a dynamic antigen-driven differentiation program initiated early during tumorigenesis. Immunity 2016;45:389–401.
49. Stronen E, Toebes M, Kelderman S, van Buuren MM, Yang W, van Rooij N, et al. Targeting of cancer neoantigens with donor-derived T cell receptor repertoires. Science 2016;352:1337–41.
50. McGranahan N, Rosenthal R, Hiley CT, Rowan AJ, Watkins TBK, Wilson GA, et al. Allele-specific HLA loss and immune escape in lung cancer evolution. Cell 2017;171:1259–71.
51. Verdegaal EM, de Miranda NF, Visser M, Harryvan T, van Buuren MM, Andersen RS, et al. Neoantigen landscape dynamics during human melanoma-T cell interactions. Nature 2016;536:91–5.
52. Rosenthal R, Cadieux EL, Salgado R, Bakir MA, Moore DA, Hiley CT, et al. Neoantigen-directed immune escape in lung cancer evolution. Nature 2019;567:479–85.
53. Kimura T, McKolanis JR, Dzubinski LA, Islam K, Potter DM, Salazar AM, et al. MUC1 vaccine for individuals with advanced adenoma of the colon: a cancer immunoprevention feasibility study. Cancer Prev Res 2013;6:18–26.